



ALMA MATER STUDIORUM
UNIVERSITÀ DI BOLOGNA

ARCHIVIO ISTITUZIONALE
DELLA RICERCA

Alma Mater Studiorum Università di Bologna
Archivio istituzionale della ricerca

Fluorogenic hyaluronan nanogels for detection of micro- and nanoplastics in water

This is the final peer-reviewed author's accepted manuscript (postprint) of the following publication:

Published Version:

Fluorogenic hyaluronan nanogels for detection of micro- and nanoplastics in water / Cingolani, Matteo; Rampazzo, Enrico; Zaccheroni, Nelsi; Genovese, Damiano; Prodi, Luca. - In: ENVIRONMENTAL SCIENCE. NANO. - ISSN 2051-8153. - STAMPA. - 9:2(2022), pp. 582-588. [10.1039/D1EN00684C]

Availability:

This version is available at: <https://hdl.handle.net/11585/873325> since: 2022-02-28

Published:

DOI: <http://doi.org/10.1039/D1EN00684C>

Terms of use:

Some rights reserved. The terms and conditions for the reuse of this version of the manuscript are specified in the publishing policy. For all terms of use and more information see the publisher's website.

This item was downloaded from IRIS Università di Bologna (<https://cris.unibo.it/>).
When citing, please refer to the published version.

(Article begins on next page)

This is the final peer-reviewed accepted manuscript of:

Fluorogenic hyaluronan nanogels for detection of micro- and nanoplastics in water

Matteo Cingolani, Enrico Rampazzo, Nelsi Zaccheroni, Damiano Genovese* and Luca Prodi*

Environ. Sci.: Nano, 2022, 9, 582

The final published version is available online at:
<https://doi.org/10.1039/D1EN00684C>

Terms of use:

Some rights reserved. The terms and conditions for the reuse of this version of the manuscript are specified in the publishing policy. For all terms of use and more information see the publisher's website.

This item was downloaded from IRIS Università di Bologna (<https://cris.unibo.it/>)

When citing, please refer to the published version.

Environmental Science Nano

Accepted Manuscript

This article can be cited before page numbers have been issued, to do this please use: M. Cingolani, E. RAMPAZZO, N. Zaccheroni, D. Genovese and L. Prodi, *Environ. Sci.: Nano*, 2022, DOI: 10.1039/D1EN00684C.



This is an Accepted Manuscript, which has been through the Royal Society of Chemistry peer review process and has been accepted for publication.

Accepted Manuscripts are published online shortly after acceptance, before technical editing, formatting and proof reading. Using this free service, authors can make their results available to the community, in citable form, before we publish the edited article. We will replace this Accepted Manuscript with the edited and formatted Advance Article as soon as it is available.

You can find more information about Accepted Manuscripts in the [Information for Authors](#).

Please note that technical editing may introduce minor changes to the text and/or graphics, which may alter content. The journal's standard [Terms & Conditions](#) and the [Ethical guidelines](#) still apply. In no event shall the Royal Society of Chemistry be held responsible for any errors or omissions in this Accepted Manuscript or any consequences arising from the use of any information it contains.

Environmental Significance Statement

View Article Online
DOI: 10.1039/D1EN00684C

This manuscript reports an attempt to face a great challenge of our times, the pollution of water resources by micro- and nanoplastics. Quantitatively, this problem is simply huge, with most of the enormous global production dispersed in the environment. Retrieving nano and micron-size fragments represents an unmet challenge, with these smaller-sized plastics also rising the highest toxicological concern.

Our strategy relies on water dispersed nanogels based on hyaluronic acid fluorescently functionalized. This nanomaterial is in a dark state in water and adheres to microplastics becoming brightly emissive. This interaction occurs with high affinity, such that even 5 nM HA-RB provides a clear analytical signal. This functionalized biopolymer has proven biocompatibility, it is water soluble and largely biodegradable.

Environmental Science: Nano Accepted Manuscript

1
2
3
4
5
6
7
8
9
10
11
12
13
14
15
16
17
18
19
20
21
22
23
24
25
26
27
28
29
30
31
32
33
34
35
36
37
38
39
40
41
42
43
44
45
46
47
48
49
50
51
52
53
54
55
56
57
58
59
60

ARTICLE

Received 00th January
20xx,**Fluorogenic hyaluronan nanogels for detection of micro- and nanoplastics in water**

Matteo Cingolani, Enrico Rampazzo, Nelsi Zaccheroni, Damiano Genovese* and Luca Prodi*

Accepted 00th January 20xx

DOI: 10.1039/x0xx00000x

Environmental pollution from plastics is exponentially increasing due to human activities. While larger microplastics can be detected with various methods, retrieving micron-size fragments and nanoplastics remains challenging. Yet, these smaller-sized plastics rise the highest toxicological concern. Here we show that a poorly emissive hyaluronan functionalized with Rhodamine B (HA-RB) adheres with high affinity to various microplastics surfaces, becoming brightly emissive. Micro- and nanoplastics (MNPs) can be successfully detected with size down to the diffraction limit of confocal microscopy (ca. 250 nm). FLIM images show that the fluorescence lifetime of the dye moieties changes according to the plastics, making possible a discrimination of the MNPs nature based on lifetime. HA-RB, compared to previous reports, eliminates false-positive results caused by formation of dye aggregates, resulting in a higher S/N ratio which allows the unequivocal detection of nano-sized fragments.

Introduction

Plastics are materials based on polymers of synthetic or semi-synthetic origin, which – since their first preparations at the beginning of last century – have now reached a central role in contemporary society with a huge global production of around 300 million tons each year.¹ Despite the increasing worldwide attention to proper disposal of plastics after their use – either by recycling, converting to energy or landfill – the large majority (ca. 70%) accumulates in the environment,¹ where it can persist for a long time. The presence of plastic debris in the environment poses a safety concern to human health owing to direct or indirect effects, and it undoubtedly disturbs ecology – intended as the interrelationships of organisms with their environment and with each other – under many aspects and thus represents a threat also for human supplies and life². The size of microplastics matters for their toxicology, with nanoplastics (overall size below 1 μm) raising the highest concern due to their direct interaction with cells. In addition, these smallest fragments are also the most difficult to detect and to eliminate. With decreasing size, plastic particles become more bioavailable to organisms: for example, micro- and nanoplastics (MNPs) have been reported in various taxa across trophic levels, such as plankton, benthic invertebrates, shrimp, bivalves, fish, seabirds.^{3,4} Furthermore, MNPs can be carriers of several kind of pollutants (heavy metals, plasticizers, etc.) or covered by biofilms, increasing even more their potentially detrimental impact on the ecosystem.

The analysis of MNPs, including the determination of their concentration, chemical nature, size distribution and morphology, remains a goal far to be fulfilled. Several analytical methods have been developed for microparticles analysis, with Fourier transform infrared (FTIR) and Raman spectroscopy and microscopy representing, at present, the gold standard for microplastics detection and analysis^{5,6}. The analysis of nanoplastics is even more challenging, with protocols still under development. Fluorescence methods – typically endowed with excellent versatility and high sensitivity, low cost and handiness of use⁷ – have found only limited application in the analysis of real samples of MNPs. Fluorescence has been used to trace dye-labelled plastic particles, or to recognize with fluorescence microscopy plastic debris after their staining with suitable dyes such as Nile Red.^{8–13} This dye has been advantageously employed to stain various microplastics in water, and also used for high-throughput techniques based on single particle tracking,¹⁴ but its tendency to aggregation causes an increase of the background signal and the occurrence of false-positive features. In addition, its affinity is relatively low towards microplastics, leading to possible desorption and thus rising additional problems.^{10–12} Very recently, more complex probes based on oligomeric silsesquioxane (POSS) derivatized with a coumarin dye were reported, which undergo an emission spectral change from yellow to blue upon the interaction with plastic particles of PS, PLA and PMMA in water.¹⁵ Inspired by previous work,¹⁶ in which we observed a strong affinity between RITC-functionalized hyaluronic acid (HA-RB) and PEGylated nanoparticles, in this contribution we investigate the onset of similar interactions between this long-chain HA functionalized with RB dyes and the surface of different MNPs dispersed in water. Such interaction provides a useful fluorescence analytical signal to highlight the presence of MNPs in water due to two overlapping effects.

^a Università di Bologna, Dipartimento di Chimica "Giacomo Ciamician", via Selmi 2, 40126, Bologna.

Electronic Supplementary Information (ESI) available: characterization of HA-RB, MNPs image microscope acquisition, image analysis. See DOI: 10.1039/x0xx00000x

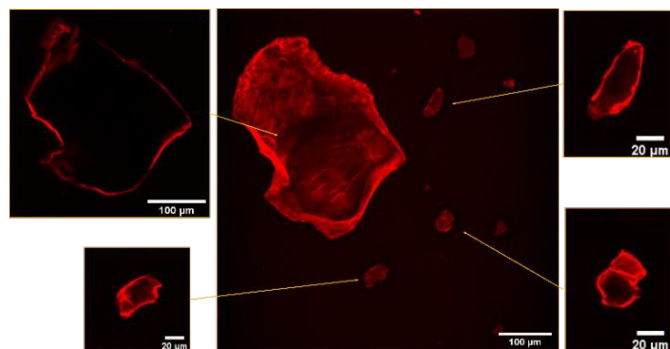


Figure 1 – Confocal fluorescence microscopy of PMMA microparticles in water, in presence of HA-RB 170 nM. Center image: overlap of 55 stacks spanning 66 micrometers in depth. The inset squares display selected individual Z-stacks showing the cross-sections of PMMA microparticles.

First, HA-RB accumulates on the surface of MNPs driven by a very high affinity; second, the fluorescence quantum yield of the RB moieties increases owing to a hydrophobicity-induced unquenching mechanism, as witnessed by the increase of their average fluorescence lifetime. Finally, the different fluorescence lifetime observed for HA-RB adsorbed on various MNPs and, in particular, on polystyrene MNPs, can provide an absolute parameter to discriminate different types of plastics.

Results and discussion

HA-RB testing for micro and nanoplastics.

HA-RB was prepared adapting a previous synthetic method.¹⁶ Briefly, HA (200-600 KDa,) was covalently functionalized with Rhodamine B isothiocyanate (RITC) in DMSO and then purified with dialysis (cut-off 12 KDa), yielding a dispersion of functionalized HA-RB in water with 1 RB moiety every ca. 60 HA monomers (1.7% doping degree of HA monomer units, i.e., \square 18 RB dyes per HA polymer chain). The yield of RITC binding to HA was obtained by measuring the absorbance of a known amount of HA-RB in a good solvent (ethanol) and using the molar extinction coefficient of RB in the same solvent.¹⁷ Native HA has an intrinsic tendency to form aggregates in water, largely driven by the rigidity of this polyanion;¹⁸ yet, the presence of RB moieties – with their hydrophobic contribution – greatly enhances this tendency and further destabilizes HA-RB polymer chains, leading to the formation of aggregated nanogels in the 100-300 nm size range.¹⁶ The role of RB dyes in promoting this aggregation in water is proved by the distinctive absorption spectrum of aggregated RB, showing a higher shoulder at 530 nm and a broader peak at 565 nm with respect to the monomeric RB dyes (see figure S1). RB moieties in the HA-RB nanogels in water suffer from heavy self-quenching, displaying an average PLQY of 0.004 and lifetime of 1.8 ns, which results in a low fluorescence background for sensing schemes both in cuvette and in fluorescence microscopy. On the contrary, HA-RB is well soluble in ethanol (whereas native HA is not), and RB moieties here display their typical absorption spectrum and bright emission (PLQY = 0.39).

We obtained water dispersed MNPs from two different sources: in a first type of samples, lab-grade microplastics were purchased by Sigma-Aldrich; in a second type, we fragmented intact, non-degraded commercial plastic objects via ball-milling and/or with a pestle and mortar. Then, each kind of MNP – in the form of a solid powder – was dispersed in distilled water, even though the dispersions were not fully stable since a large part of the MNPs fragments separated either by precipitation or by floating on the water surface. To these heterogeneous dispersions, a small volume of HA-RB in water was added (typically 50 μ L to 1 mL of MNP dispersion), yielding a final concentration of HA-RB \square 170 nM (estimated concentration of polymer chains, using 400 KDa as the MW). After shaking for 30 seconds, the MNP dispersions were ready for fluorescence microscopy observations, performed on a drop of 50 μ L of the dispersion deposited on a coverglass.

As readily observed by confocal fluorescence microscopy under 561 nm excitation, after mixing with HA-RB, MNPs become bright luminescent in the 590 \pm 30 nm range. Confocal images (Figure 1) show that MNPs are effectively labelled and clearly distinguishable from the background both when the fragments are very large (with a few fragments reaching up to 100 microns in diameter) and when the fragments are about 1 micron in diameter (Figure S8). Confocal sectioning with an oil immersion, high numerical aperture objective (NA=1.45, magnification 100x) allows to confirm that HA-RB labelling is a surface process, and that no penetration of HA-RB in the MNPs occurs, as proven by the dark inner part of the MNPs, which on turn display a bright fluorescent surface (Figure 1).

Comparison of the same MNPs samples treated with Nile Red (NR), a standard fluorescent dye in available fluorescence-based techniques for microplastic detection, reveals a comparable intensity onto the surface of MNPs owing to NR adsorption, but also a relevant amount of NR aggregates with different sizes, from sub-micron to several tens of micrometers, that provide “false positive” fluorescent objects, as also previously reported.¹⁹ These NR aggregates can be distinguished from MNPs only via lifetime imaging analysis, owing to their short lifetime (figure S4).

Yet, in these conditions and without any purification step, the reference sample of HA-RB in water, in absence of MNPs, contains small (< 500 nm diameter) and poorly emissive HA-RB aggregates. The presence of nanogels of HA-RB in this size range impedes the unambiguous recognition of nanoplastics of similar size, even if they do not interfere with the identification of microplastics with diameter larger than ca. 1-2 micron. To overcome this issue and allow for clear recognition also of nanoplastics with size smaller than 1 micron, we added a centrifugation step (5000 rpm, 10 minutes) that separates MNPs fragments, while non-adsorbed HA-RB nanogels – owing to their small size, hydration and density – remain in the supernatant and are eliminated. In absence of MNPs, with this additional purification step, we could not identify any emissive aggregate (figure S7). Therefore, also sub-micron emissive features in the MNP samples, when treated with this centrifugation step, can be explicitly attributed to nanoplastics with size down to the resolution of the microscope (ca. 250 nm).

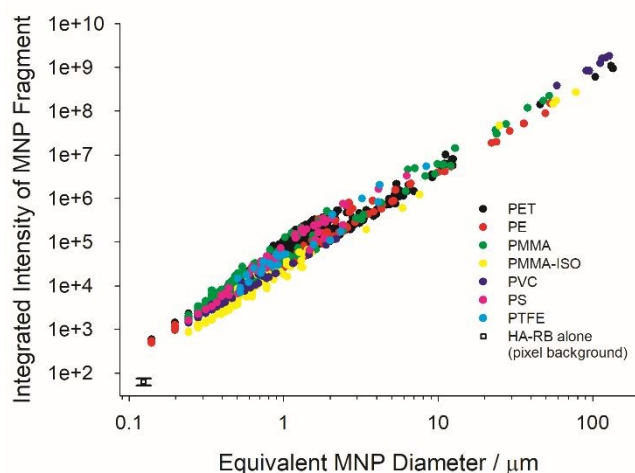


Figure 2 – Plot of integrated pixel intensity versus the size (equivalent diameter, calculated from the area of the fragments $d=(A/2\pi)^{0.5}$) of the MNP fragment.

We acquired large images of $5.5 \times 5.5 \text{ mm}^2$ (multi-frame mosaic acquisitions of 10×10 images at constant height from the coverglass surface, in the range 5-50 microns from surface) of MNPs samples labelled with HA-RB. To best observe fluorescently stained MNP samples we immersed them in a hyaluronan hydrogel (16 mg/mL native HA 200-600 KDa in water) rather than pure water, in order to slow down water evaporation and movement of fragments during acquisition. Native hyaluronan was selected – among other hydrogels – because it does not interfere with the photophysical properties of HA-RB and with its interaction with MNP fragments (Figure S2). We then analysed the confocal images with a particle tracking routine based on ImageJ, which selects particles based on an intensity threshold value taken well above background noise (e.g., threshold = ca. 500 counts for background signal = 64 ± 12 counts, detailed description in Supporting Information and Figures S7-S8). Plotting the integrated pixel intensity versus the size (equivalent diameter) of the MNP fragment shows that, as expected, the overall fluorescence signal builds up in fragments with increasing size (Figure 2). The sub-micron part of the plots reveals that a large number of nanoplastics are brightly labelled with HA-RB and that they stand out of the background with an overall intensity which is from ≈ 10 to >200 times the background noise. In a log-log plot the intensity shows a clear linear trend, well fitted with a slope close to 2, as expected for a surface adsorption process. The slightly larger slope than 2 points at the presence of rough surfaces with higher fractal dimension.²⁰ From the fitting we can calculate the intensity of a nanoplastic fragment of size corresponding to a single pixel (square pixel of side 124 nm), which allows a ready comparison with the background, showing that MNPs stained with HA-RB display between 3.5 (PMMA-iso) and 7.4 times (PMMA) the average intensity of background for 124 nm size (table 1). We compared these results with the use of molecular dye Rhodamine B (RB), which is soluble in water. RB shows good

affinity towards MNPs surface, with high luminescence from the microplastics fragments. Yet, RB is highly emissive also in water, therefore the high signal from the solution hinders the possibility to detect the small nanoplastic fragments.

Table1 – Fitting parameters of the plot shown in figure 2. The log-log datapoints have been fitted with a linear fit, the table reports intercept (i.e., $\log(I)$ at diameter = $10^0 \mu\text{m}$), slope and calculated intensity (and $\log(I)$) at single pixel (square of lateral size 124 nm), which is compared with the average background intensity at single pixel.

	Intercept	Slope	Intensity ($\log I$) at single pixel
PS	4.75	2.43	352 (2.55)
PTFE	4.67	2.25	422 (2.63)
PMMA	4.64	2.17	472 (2.67)
PMMA-iso	4.35	2.19	229 (2.36)
PVC	4.51	2.24	300 (2.48)
PE	4.54	2.12	398 (2.60)
PET	4.64	2.25	416 (2.62)
Background	--	--	64 ± 12 (1.81)

Fluorescence lifetime imaging of MNPs using HA-RB.

The variation of the excited state lifetime of RB moieties upon interaction with MNPs was also investigated. As previously found, the lifetime of HA-RB in water is short and multiexponential, corresponding to a broadly self-quenched state. Interestingly, the average lifetime displays relevant variations upon interaction with MNPs, pointing to a conformational change of HA-RB nanogels with a fraction of self-quenched RB moieties becoming emissive from a monomeric-like state.

In particular, at low concentrations of HA-RB, the fluorescence decay of HA-RB onto MNPs surface appears longer and in some cases also more similar to a single-exponential decay with respect to the HA-RB nanogels in water (Figure S3). This can be explained by a hydrophobicity-induced unquenching mechanism: breaking of the RB dimers and aggregates (responsible for the initial self-quenching and for HA-RB aggregation as nanogels) occurs due to conformational changes of HA-RB upon adsorption on MNP surface, which results in the local increase of the average lifetime, narrowing of the lifetime distribution and, consequently, in the enhancement of the fluorescence quantum yield. Yet, the conformational changes appear to be quite sensitive to the type of surface, so that different degrees of lifetime increase are observed for different types of MNPs. Therefore, it is noteworthy to underline that, in these conditions, the chemical nature of MNPs can be made evident via FLIM analysis, allowing for a straightforward distinction as shown in figure 3 for PS and PMMA microplastics, which can be clearly recognized even when mixed together.

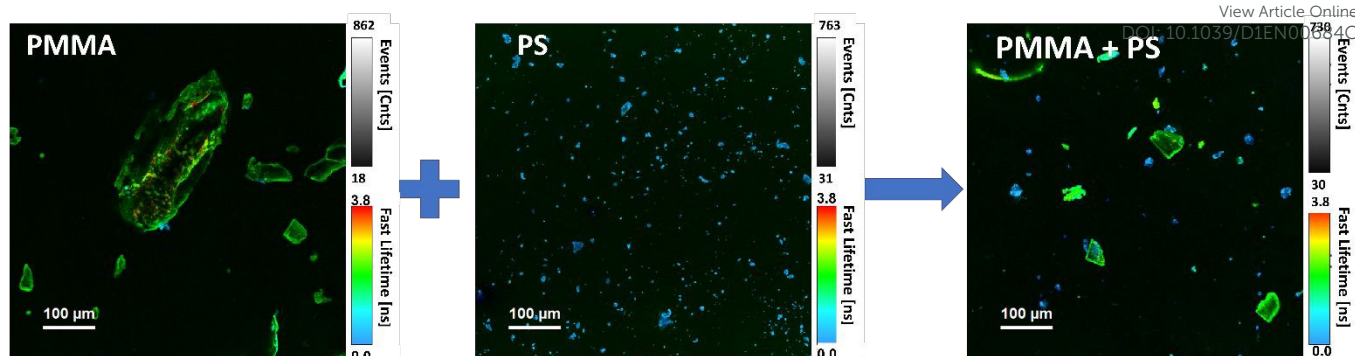


Figure 3 – FLIM microscopy images of PMMA and PS MNPs labelled with HA-RB, before and after mixing the two samples.

The lifetime dependence on the specific plastic surface could be explained by the interplay of two different interactions: the first is the hydrophobic interaction, which causes the increase of lifetime, and which characterizes the binding of HA-RB onto surfaces of purely hydrophobic plastics such as PTFE and PVC. The second interaction that can play a role on the affinity with MNP surfaces is the H-bond formation due to the hyaluronan functional groups of HA-RB, which may be more relevant in the binding with less hydrophobic surfaces of PMMA and PET MNPs. PS appears as a singular case, in which electronic interactions with the styrene units may be at the basis of the short and approximately monoexponential lifetime of HA-RB.

Yet, the build-up of HA-RB layers on MNPs surface, at higher HA-RB concentration, changes again the photophysics of the RB moieties. Local intensity on the surface of MNPs increases, but the emission decay gradually becomes shorter and multiexponential. The additional HA-RB on the surface of MNPs indeed increases the local density of RB dyes and therefore the probability of self-quenching interactions among RB moieties is enhanced, resulting in the observed shorter and multiexponential lifetime (Figure 4). For these reasons, a low concentration of HA-RB should be used for discriminating among the different kinds of plastics; this concentration is however highly sufficient to give a clear image (Figures S3 and S6).

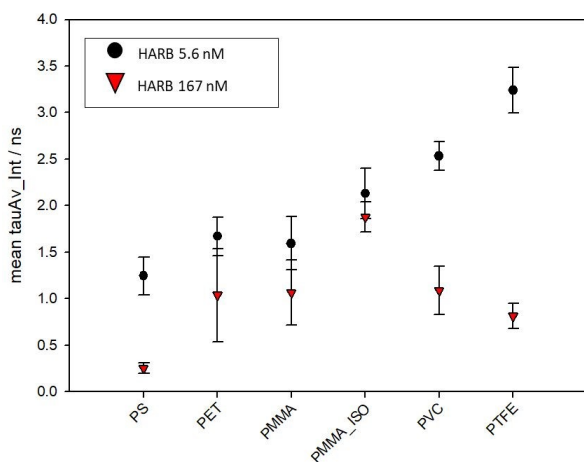


Figure 4 – Mean values with standard deviations of “ τ_{Av_Int} ”, i.e., the average lifetime weighted on intensity, for MNPs samples incubated with HA-RB 170 nM (red triangles) and HA-RB 5.6 nM (black circles).

The ability of HA-RB to readily stain micro and nanoplastics even at extremely low concentration ($\square 5$ nM of polymer chain and $\square 100$ nM Rhodamine B dyes, to be compared with the typical concentration used for tests based on Nile Red, in the range 1-10 μ M) can be explained by the concomitant effect of a high affinity of the HA-RB nanoprobe towards many plastic surfaces, and by high PLQY due to the effective switch-ON of the luminescence of RB moieties upon adhesion of the probe onto these surfaces.

Conclusions

In conclusion, we report here a fluorogenic material, i.e., hyaluronic acid functionalized with Rhodamine B (HA-RB), with a very weak fluorescence intensity in water, but which readily adsorbs onto the surface of various MNPs with a concomitant enhancement of brightness, making them fluorescent. Fluorescently stained MNPs are clearly visible with size down to the resolution of a confocal microscope, with nanoplastics fragments of approximately 250 nm standing out of the background. This high sensitivity can be achieved due to the recovery of the fluorescence quantum yield of the RB moieties thanks to a hydrophobicity-induced unquenching together with a high affinity interaction with MNPs. These properties allow for MNP detection even at a very low concentration of the probe ($\square 5$ nM). Furthermore, the lifetime parameter reveals a different degree of hydrophobicity induced unquenching of HA-RB on the surface of different microplastics, making possible the identification of the type of MNPs based on their fluorescence lifetime.

These results represent a feasibility study, in controlled conditions, and its applicability to real MNPs debris in environmental samples remains a challenge. The intrinsic versatility of the reported fluorogenic hyaluronan, though, represents a valuable strength: in fact, various properties of fluorogenic hyaluronan nanogels can be finely tuned by changing the mass, the derivatization or even the chemistry of HA and of the fluorogenic moiety. This versatility is potentially very advantageous to design custom probes for different applications, in which sensitivity requires proper balance with selectivity towards various categories of interferents and with different experimental conditions.

Experimental

Synthetic procedure

Synthesis of HA-RB was adapted from a previously reported procedure.¹⁶ Briefly, HA (200-600 kDa, 30 mg) was dispersed in DMSO (8 mL) and Rhodamine B isothiocyanate (RITC, 4.4 mg) was added under stirring; the reaction was left to proceed for 24h at room temperature. The product was then diluted with water (8 mL) and unreacted RITC was eliminated via dialysis (at least 3 days room T, regenerated cellulose, cut-off 12 kDa), to finally obtain a dispersion of functionalized HA-RB in water with 1 RB moiety every ca. 60 HA monomers (1.7% doping degree of HA monomer units, i.e., \square 18 RB dyes per HA polymer chain).

Materials and methods.

Lab-grade plastics were either purchased from Sigma Aldrich ("PS", Polystyrene 9003-53-6; "PET", Poly (ethylene terephthalate) 25038-59-9; "PMMA_ISO", Poly(methyl methacrylate)-isotactic 25188-98-1; "PVC", Poly(vinyl chloride, 9002-86-2; "PTFE" Poly(tetrafluoroethylene) 9002-84-0; "PE", Polyethylene 9002-88-4) or obtained by grinding clean and new plastics objects ("PMMA" Poly(methyl methacrylate) from ball-mill grinded disposable fluorescence cuvette). PET and PMMA shows macroscopic/granular fragments and were grinded with an analytical mill IKA A10 Basic until a fine powder was obtained. The other microplastic samples were already in powder form and were finely grinded in a mortar to further reduce mesh size and increase the fraction of nanoplastics and small microplastics.

Scanning Electron Microscopy

Scanning Electron Microscopy (SEM) was carried out by using a Philips 515 microscope at an accelerating voltage of 15 kV, on samples fixed with a conducting bi-adhesive tape on an aluminium stub and coated with gold. Images were analysed with Image J software.

Sample preparation for fluorescence imaging

MNPs samples were weighted and incubated under mechanical agitation with 1 mL of water solution containing HA-RB 170 nM. After that, 30 μ L of the MNP dispersion were mixed together with a drop of 100 μ L hyaluronan hydrogel (16 mg/mL) directly on the glass slide. This solution volume assures that the hydrogel drop remain viscous during the experiments, to homogeneously disperse the sample and to delay evaporation. The same procedure has been used to incubate microplastics with Nile Red. In the second set of experiments, we added a purification procedure. Two set of each microplastic sample were incubated in glass vials under mechanical agitation for 30 min with 1 mL of water solution of 170 nM HA-RB for one set and 5.6 nM HA-RB for the other one. After the incubation, 2 mL of water were added to each vial and then centrifuged at 5000 rpm for 10 min. This process separates MNPs fragments, while non-adsorbed HA-RB nanogels remain in the supernatant and 2 mL of it is carefully eliminated with a Pasteur pipette. Then 2 mL

of new water was added to each sample and centrifuged again. This washing process was repeated three times. Finally, we mixed the centrifuged MNPs with HA hydrogel for confocal and FLIM imaging.

Photophysical characterization

Confocal and FLIM

Confocal images were registered on a Nikon A1R microscope with an oil immersion, high NA objective (NA=1.45, magnification 100x), an excitation laser at 561 nm and a GaAsP PMT with emission filter at 595/50nm. The acquisition parameters were set to 1 A.U., 8x Signal Average, Resonant Scanning Mode, Laser Power=1.64%, PMT GaAsP HV=70. This setting was kept the same for all the samples analyzed. To obtain large statistic ensembles of MNPs we acquired 10x10 mosaic captures, with a final field of view of 1.2 x 1.2 mm² and single pixel size of 124 nm.

FLIM images were acquired with a time-correlated single photon counting (TCSPC) system of Picoquant GmbH Berlin, using a 405 nm pulsed excitation laser at 10 MHz repetition rate, a 560 nm long-pass emission filter, a Hybrid PMA detector and a Picoquant PicoHarp 300 correlation board. FLIM images were then analysed with SymPhoTime 64, PicoQuant GmbH.

Image analysis

Confocal images of the different samples have been analysed with a particle tracking macro based on ImageJ commands. The macro was written to process large images with comparable conditions and to obtain relevant information on all the fragments in the area. It processes images to find particles with size greater than the pixel size (124 nm) and pixel intensity higher than a pre-set threshold. The output includes area, minimum, maximum and mean pixel intensities together with the integral of the identified area. Additional detailed information and examples on the image analysis process can be found in Supporting Information.

Author Contributions

Methodology, Software, Data curation: M.C., D.G.; Supervision: E.R., D.G., N.Z.; Conceptualization and supervision: E.R., D.G., N.Z., L.P.; Funding acquisition: D.G. and L.P.; Writing – original draft, review & editing: all authors contributed equally.

Conflicts of interest

There are no conflicts to declare.

Acknowledgements

This work is supported by University of Bologna ("Almaldea" initiative) and by the Italian Ministero dell'Istruzione, Università e Ricerca, MIUR (Project PRIN 2017EKCS35).

References

- 1 M. Enfrin, L. F. Dumée and J. Lee, Nano/microplastics in water and wastewater treatment processes – Origin, impact and potential solutions, *Water Res.*, 2019, **161**, 621–638. 14
- 2 A. Ragusa, A. Svelato, C. Santacroce, P. Catalano, V. Notarstefano, O. Carnevali, F. Papa, M. C. A. Rongioletti, F. Baiocco, S. Draghi, E. D'Amore, D. Rinaldo, M. Matta and E. Giorgini, Plasticenta: First evidence of microplastics in human placenta, *Environ. Int.*, 2021, **146**, 106274. 15
- 3 W. J. Shim, S. H. Hong and S. E. Eo, Identification methods in microplastic analysis: a review, *Anal. Methods*, 2017, **9**, 1384–1391. 16
- 4 https://ec.europa.eu/environment/marine/good-environmental-status/descriptor-10/pdf/GESAMP_microplastics%20full%20study.pdf, https://ec.europa.eu/environment/marine/good-environmental-status/descriptor-10/pdf/GESAMP_microplastics%20full%20study.pdf. 17
- 5 A. Käßler, D. Fischer, S. Oberbeckmann, G. Schernewski, M. Labrenz, K. J. Eichhorn and B. Voit, Analysis of environmental microplastics by vibrational microspectroscopy: FTIR, Raman or both?, *Anal. Bioanal. Chem.*, 2016, **408**, 8377–8391. 18
- 6 C. Fang, Z. Sobhani, X. Zhang, L. McCourt, B. Routley, C. T. Gibson and R. Naidu, Identification and visualisation of microplastics / nanoplastics by Raman imaging (iii): algorithm to cross-check multi-images, *Water Res.*, 2021, **194**, 116913. 19
- 7 A. Credi and L. Prodi, Inner filter effects and other traps in quantitative spectrofluorimetric measurements: Origins and methods of correction, *J. Mol. Struct.*, , DOI:10.1016/j.molstruc.2014.03.028. 20
- 8 J. C. Prata, V. Reis, J. T. V. Matos, J. P. da Costa, A. C. Duarte and T. Rocha-Santos, A new approach for routine quantification of microplastics using Nile Red and automated software (MP-VAT), *Sci. Total Environ.*, 2019, **690**, 1277–1283.
- 9 L. Lv, J. Qu, Z. Yu, D. Chen, C. Zhou, P. Hong, S. Sun and C. Li, A simple method for detecting and quantifying microplastics utilizing fluorescent dyes - Safranin T, fluorescein isophosphate, Nile red based on thermal expansion and contraction property, *Environ. Pollut.*, 2019, **255**, 113283.
- 10 G. Erni-Cassola, M. I. Gibson, R. C. Thompson and J. A. Christie-Oleza, Lost, but Found with Nile Red: A Novel Method for Detecting and Quantifying Small Microplastics (1 mm to 20 µm) in Environmental Samples, *Environ. Sci. Technol.*, 2017, **51**, 13641–13648.
- 11 T. Maes, R. Jessop, N. Wellner, K. Haupt and A. G. Mayes, A rapid-screening approach to detect and quantify microplastics based on fluorescent tagging with Nile Red, *Sci. Rep.*, 2017, **7**, 44501.
- 12 W. J. Shim, Y. K. Song, S. H. Hong and M. Jang, Identification and quantification of microplastics using Nile Red staining, *Mar. Pollut. Bull.*, 2016, **113**, 469–476.
- 13 A. I. Catarino, A. Frutos and T. B. Henry, Use of fluorescent-labelled nanoplastics (NPs) to demonstrate NP absorption is inconclusive without adequate controls, *Sci. Total Environ.*, 2019, **670**, 915–920. DOI: 10.1039/C9EM00684C
- R. Molenaar, S. Chatterjee, B. Kamphuis, I. M. J. Segers-Nolten, M. M. A. E. Claessens and C. Blum, Nanoplastic sizes and numbers: quantification by single particle tracking, *Environ. Sci. Nano*, 2021, **8**, 723–730.
- R. Nakamura, H. Narikiyo, M. Gon, K. Tanaka and Y. Chujo, An optical sensor for discriminating the chemical compositions and sizes of plastic particles in water based on water-soluble networks consisting of polyhedral oligomeric silsesquioxane presenting dual-color luminescence, *Mater. Chem. Front.*, 2019, **3**, 2690–2695.
- F. Palomba, E. Rampazzo, N. Zaccheroni, M. Malferrari, S. Rapino, V. Greco, C. Satriano, D. Genovese and L. Prodi, Specific, Surface-Driven, and High-Affinity Interactions of Fluorescent Hyaluronan with PEGylated Nanomaterials, *ACS Appl. Mater. Interfaces*, 2020, **12**, 6806–6813.
- J. M. Dixon, M. Taniguchi and J. S. Lindsey, PhotochemCAD 2: A Refined Program with Accompanying Spectral Databases for Photochemical Calculations, *Photochem. Photobiol.*, 2005, **81**, 212.
- C. E. Reed, X. Li and W. F. Reed, The effects of pH on hyaluronate as observed by light scattering, *Biopolymers*, 1989, **28**, 1981–2000.
- T. Stanton, M. Johnson, P. Nathanail, R. L. Gomes, T. Needham and A. Burson, Exploring the Efficacy of Nile Red in Microplastic Quantification: A Costaining Approach, *Environ. Sci. Technol. Lett.*, 2019, **6**, 606–611.
- C. A. Brown, W. A. Johnsen, R. M. Butland and J. Bryan, Scale-Sensitive Fractal Analysis of Turned Surfaces, *CIRP Ann.*, 1996, **45**, 515–518.